# Journal Pre-proof

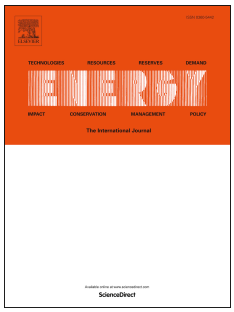

Performance and emissions of hexanol-biodiesel fuelled RCCI engine with double injection strategies

Justin Jacob Thomas, G. Nagarajan, V.R. Sabu, C.V. Manojkumar, Vikas Sharma

PII: S0360-5442(22)00972-0

DOI: https://doi.org/10.1016/j.energy.2022.124069

Reference: EGY 124069

To appear in: *Energy*

Received Date: 12 October 2021

Revised Date: 31 March 2022

Accepted Date: 20 April 2022

Please cite this article as: Thomas JJ, Nagarajan G, Sabu VR, Manojkumar CV, Sharma V, Performance and emissions of hexanol-biodiesel fuelled RCCI engine with double injection strategies, *Energy* (2022), doi: https://doi.org/10.1016/j.energy.2022.124069.

## CRediT author statement

**Justin Jacob Thomas:** Conceptualization, methodology, investigation, validation, formal analysis, writing - original draft

**Nagarajan G:** Writing – review and editing, supervision

**Sabu VR:** Resources, methodology, writing – review and editing

**Manojkumar CV:** Software, resources

**Vikas Sharma:** Investigation, Formal Analysis

# Performance and Emissions of Hexanol-Biodiesel fuelled RCCI engine with double injection strategies

*Justin Jacob Thomas*[*a], *Nagarajan G*[a], *Sabu VR*[a], *Manojkumar CV*[a], *Vikas Sharma*[b]

[a] Department of Mechanical Engineering, CEG Campus, Anna University, Chennai 25, Tamil Nadu, India
[b] Department of Mechanical Engineering & Design, Aston University, Birmingham B4 7ET, United Kingdom

## ABSTRACT

In the present work, an attempt has been made to operate a low-temperature reactivity controlled compression ignition (RCCI) engine using fuel produced from agro/food industry waste. Biodiesel produced from residual cooking oil (RCOB) and n-hexanol has been used as high reactivity fuel (HRF) and low reactivity fuel (LRF) respectively, in a modified diesel engine. The engine was operated at mid-load and 1500 rpm with RCOB injected in-cylinder at higher injection pressures ($P_{inj}$) of 400 to 600 bar whereas hexanol was injected into the inlet manifold at a lower $P_{inj}$ of 3 bar. The proportion of Hexanol to RCOB was varied from 20% to 50%. Two injection pulses per cycle were used for injection of RCOB and the injection timing, duration, and fuel quantity were varied whereas hexanol injection was maintained constant at 355 ° bTDC. The injection parameters, along with exhaust gas recirculation (EGR) were optimized for the lowest smoke and NO emissions. It was observed that smoke and NO emissions reduced with late main injection, whereas smoke increased and NO reduced with advanced pilot injection. The test engine was operated at these optimized conditions and the combustion and emission data were collected and compared to that of a single injection of HRF. A maximum reduction in NO emissions by 96% and smoke emission by 80% were observed with 25% EGR. The increase of 1% in indicated thermal efficiency is an added benefit.

**Keywords**: RCCI, Hexanol, Residual cooking oil biodiesel, EGR, Double injection

## Nomenclature

| | |
|---|---|
| ASTM | American Society For Testing And Materials |
| aTDC | After Top Dead Centre |
| ETS | Exhaust Treatment System |
| °bTDC | Degree Before Top Dead Centre |
| CA | Crank Angle |
| CD | Combustion Duration |
| CI | Compression Ignition |
| CO | Carbon Monoxide |
| EGR | Exhaust Gas Recirculation |
| EU | European Union |
| EV | Electric Vehicle |
| HC | Hydrocarbon |
| HCCI | Homogenous Charge Compression Ignition |
| HRF | High Reactivity Fuel |
| HRR | Heat Release Rate |
| ICE | Internal Combustion Engine |

| | |
|---|---|
| ID | Ignition Delay |
| IMEP | Indicated Mean Effective Pressure |
| KOH | Pottasium Hydroxide |
| LPG | Liquified Petroleum Gas |
| LRF | Low Reactivity Fuel |
| LTC | Low-Temperature Combustion |
| NO | Nitric Oxide |
| $P_{inj}$ | Injection Pressure |
| PCCI | Premixed Charge Compression Ignition |
| PFI | Port Fuel Injection |
| RCCI | Reactivity Controlled Compression Ignition |
| RCO | Residual Cooking Oil |
| RCOB | Residual Cooking Oil Biodiesel |
| SI | Spark Ignition |
| SOC | Start Of Combustion |
| SOI | Start Of Injection |

*Corresponding Author Email : justinjacobthomas@gmail.com

| | | | |
|---|---|---|---|
| TDC | Top Dead Centre | US | United States |

## 1. INTRODUCTION

With the rapid increase in the automotive market, urban air quality, as well as national energy security, is deteriorating. The exhaust gases during idling from a conventional internal combustion engine (ICE) can cause nausea, breathing trouble, cardiac arrest, or even death (Rahman et al., 2013). In 2018, the $CO_2$ emissions for China, the US, EU, and India were 10, 5.41,4.39, and 2.65 billion tonnes respectively, 30% of which comes from the transportation sector (Hindu, 2020). The European Commission is targeting a reduction in $CO_2$ emissions by 15%, by 2025 and at the same time, the upcoming emission norm (Euro VII) will impose a reduction in NO and soot emission by 50% compared to current Euro VI norms (Garcia, 2020). As such, this demands a simultaneous reduction in NOx, smoke, and $CO_2$ emissions. Electric vehicles (EVs) provide a promising solution to the emission problem and at the same time improve the energy security of the country, given that electrical power is generated via renewable energy sources. The total $CO_2$ emissions over an EVs full life depends on the power source used at the location where the vehicle is manufactured and operated. Considering life cycle assessment, $CO_2$ emissions from EVs are 59% higher than those from ICE vehicles (Goel et al, 2021). As a result, in a nation like India, where over 80% of electricity is generated by fossil fuels, EVs lose their advantages.

ICE operating in CI (compression ignition) mode involves a trade-off between $CO_2$, NOx, and smoke emissions, and as a result, they cannot all be reduced simultaneously. (Reijnders et al., 2016). Though the efficiency of Diesel ICE is comparatively higher than gasoline ICE, the increased NOx and smoke emissions emitted require costly exhaust-treatment systems (ETS) which adds to the automobile's total cost (Guan et al., 2013). Low-temperature combustion (LTC) on the other hand can reduce these three emissions simultaneously (Benajes et al, 2018). The LTC method employs combustion techniques, such as exhaust gas recirculation, earlier multiple injections (Papagiannakis *et al.*, 2017) together with combustion chamber optimization to reduce the necessity of ETS.

Among the various LTC strategies such as HCCI, PCCI and RCCI; RCCI (reactivity controlled CI) has been shown to improve combustion process control by changing the charge reactivity inside the cylinder (Zehni et al., 2017). Within the cylinder, a mixture of two fuels with varying reactivities is created. The low reactivity fuel (LRF) is inducted into the inlet port during early suction stroke whereas the high reactivity fuel (HRF) is injected into the combustion chamber during compression stroke (Kokjohn, 2011). RCCI combustion is capable of operating at a wide range of engine loads (4.6-14.6 bar) while emitting low NOx and smoke and achieving a greater thermal efficiency (Kokjohn & Reitz, 2013). Curran et al (2012) compared RCCI operation on a light-duty diesel engine to CDC operation and observed that the thermal efficiency increased by 7% compared to Diesel operation, NOx emissions reduced whereas HC and CO emission increased. It was understood that the enhancement in thermal efficiency and lower fuel intake, was a result of decreased heat losses. Dempsey et al. (2013) operated an RCCI engine with methanol/diesel and gasoline/diesel and discovered that using alcohol fuel

may increase engine load without requiring EGR, while gasoline/Diesel combination requires EGR at higher loads (>7 bar IMEP). Li et al. (2015) conducted a computational analysis of the impacts of gasoline and biodiesel fuels on RCCI combustion and discovered that gasoline/biodiesel produced less NOx than straight biodiesel. Mohsin et al (2014) demonstrated that biodiesel may be utilized in a dual-fuel engine without major modification to Diesel engine. Gharehghani et al (2015) observed a more stable cycle to cycle operation with natural gas/biodiesel fuelled RCCI compared to natural gas/Diesel due to higher cetane number and presence of in-fuel oxygen. While NOx and smoke emissions have decreased, since the $CO_2$ emission is proportional to fuel consumption, the need is to move from traditional non-renewable fuels to carbon-neutral renewable fuels to meet the normative. Biofuels such as biodiesel, bio alcohol are alternatives for propulsion in this regard.

Biodiesels are esters of long-chain fatty acids that are produced from animal fats, vegetable oils and are refined to meet the ASTM standards for Diesel fuel (Wiznia et al. 2006). However, the hurdle with biodiesel is the higher price of raw oil which increases the overall cost of the fuel in comparison to fossil diesel (Wei *et al.*, 2018). The utilization of waste resources as feedstock for biodiesel preparation can help in this regard. Residual cooking oil (RCO) is essentially a surplus or residue and therefore the use of RCO as an energy source lowers the total cost of the fuel (Aboelazayem *et al.*, 2018). In more than 70% of the households, RCO is improperly disposed into kitchen or other sinks and eventually into the sewage system. This is primarily because there is no widespread collection system in place (Tsoutsos *et al*., 2019). This RCO being poured into drains and sewers contaminates water supplies as well as creates issues for treatment plants. RCO in sewage systems can lead to blockage and flooding of sewers which can lead to pollution of nearby water resources (Wallace *et al*., 2017). RCO, as it is insoluble and has a lower rate of decomposition, escapes the treatment facility and pollutes the land and water resources (Ramos *et al.*, 2013). Therefore recycling RCO into biodiesel not only contributes in terms of renewability of fuel but also solves the issue of waste disposal.

Similarly, alcohol fuels are considered as an alternative to petroleum-based fuel because of the presence of fuel-bound oxygen which enhances the mixture formation and hence reduces smoke and hydrocarbon (HC) emissions (Lu et al, 2004). Bio-alcohols can be produced from carbon-based agricultural feedstocks (sugarcane, rice straw, corn stalks) (Rakopoulos *et al.*, 2019). Stubble burning after harvest is a major concern in India especially in northern states where agriculture is the main economy. After the harvest, an estimate of 500 million tonnes of crop residues is burnt in Indo-Gangetic plain (Sharma *et al*., 2010). The PM2.5 (particulate matter with size less than 2.5 μ) levels at Delhi in 2017 were 710 $\mu g/m^3$ with the Air Quality Index of 999 (>100 is unhealthy, >300 is hazardous) (Chaitanya, 2018). In contrast, agricultural wastes such as rice straw, corn stalk, or forest biomass wastes such as wood pulp, paper mill waste, can be converted into bio-alcohols, such as hexanol. Therefore, the production of hexanol is not only renewable but solves a big environmental issue faced by the country today.

Lower alcohols such as methanol or ethanol have a lower energy density, lower cetane number and higher latent heat, leading to difficulty in auto-ignition compared to higher (>C4) alcohols (Karabektas & Hosoz, 2009, Zhong et al., 2022). Additionally, the poor miscibility with mineral Diesel and poor lubricating property is a hindrance towards use in CI engines (Campos-

Fernandez et al, 2012). Hexanol is a straight-chain alcohol with 6 C atoms produced from agricultural residue. It is a colourless liquid and is miscible with mineral Diesel and has a greater calorific value and cetane number than all lower alcohols (Thomas et al, 2021).

Guan et al (2017) compared the effects of residual cooking oil biodiesel (RCOB)/liquefied petroleum gas (LPG) and Diesel/LPG on combustion as well as emission in a 4-cylinder CI engine. While RCOB/LPG decreased smoke emissions in dual-fuel mode, NOx emissions rose in comparison to Diesel/LPG. Atmanli (2016) compared the effect of Diesel (D), RCOB, propanol (Pr), butanol (Bn), pentanol (Pn) blends in a diesel engine. The addition of higher alcohols improved the cloud point and cold flow plug point of the D-RCOB mix, though density, heating value, cetane number, and viscosity were reduced. Alcohol blends produced less NOx than diesel and the impact on $NO_x$ emissions increased with increasing carbon. CO emissions, on the other hand, rose for all alcohol mixes. Ma et al. (2017) used a constant volume chamber to examine the impact of n-pentanol blending to RCOB in ratios of 0,20, 40% (by volume) on spray properties, ignition, and combustion. The results suggested that the liquid length reduced with increasing temperature. An increase in the proportion of pentanol also promoted the ignition timing. Additionally, it was found that the addition of pentanol resulted in a reduction in soot emissions.

Kumar et al. (2016) did a comparative analysis of diesel-alcohol blends' effect on engine performance. Four blends comprising 30% (volume) of $C_4$, $C_5$, $C_6$ and $C_8$ alcohol with diesel fuel were investigated. Ignition delay (ID) decreased with increasing the C atom in the alcohol. Combustion duration (CD) showed the opposite trend and increased with increasing C atoms. $NO_x$ emission reduced for all blends at lower loads whereas it increased for pentanol and hexanol at rated load. Smoke and CO emissions reduced with an increase in C atoms in the alcohol and were lower in comparison to diesel. Victor et al. (2017) studied the use of 1-Hexanol in a CI engine by mixing it with diesel in percentages of 10, 20, and 30 (by volume). Tests were conducted on a single-cylinder constant speed engine. The results indicated that adding hexanol to diesel resulted in a prolonged ID, resulting in increased heat release rate (HRR) and pressure. Smoke emissions decreased as the percentage of hexanol rose, but NOx emissions increased.

Qian et al. (2015) studied RCCI operation with Diesel-gasoline and Diesel-ethanol in a 1-cylinder engine. It was witnessed that ID increased for ethanol-diesel combination whereas the temperature and pressure dropped with increased premixed fraction. With increased premixed fraction, $NO_x$ and Smoke were reduced. HC emissions from Diesel-ethanol were greater than from Diesel-gasoline. Benajes et al. (2015) explored the effects of LRF and its ratio on a heavy-duty diesel engine using different fuel blends: E85, E20-95, E10-98 and E10-95. Tests were performed on a 1-cylinder heavy-duty CI engine at 1200 rpm and constant CA50 at 5 °bTDC. Results showed that the in-cylinder reactivity gradient affected engine efficiency. A reduced gradient improved the indicated efficiency by about 4.5%. NOx and smoke emissions were lesser than Euro VI standards and CO, HC emission was also lower than high reactivity gradient fuels.

From the review of the available literature, it is evident that both RCOB and higher alcohols are suitable alternatives for petroleum-based fuels in CI engines. However, most of the works

available in the literature are about the use of these fuels in blended form along with Diesel or Gasoline. Neat alcohol fuels are restricted to SI engines because of their physicochemical properties. The studies available on RCCI combustion were also limited to traditional fuels and their blends with lower alcohol or biodiesel. Investigations on higher alcohol fuel (hexanol) in neat form or LTC were not available at the time of the present work. Therefore the present investigation would provide insight into the combustion of RCOB and hexanol in a RCCI engine.

In the present work, RCOB and hexanol, both of which are renewable fuels produced from agro wastes, were utilized as LRF and HRF in a RCCI engine. Hexanol was injected into the inlet port during early suction stroke whereas RCOB was injected directly into the combustion chamber during the compression stroke. Base readings were taken with Diesel and RCOB/hexanol with a single injection of HRF (Thomas et al, 2020). Thereafter, exhaust gas recirculation and injection parameters for double injection (pilot and main injection) such as timing, quantity, and pressure were experimentally optimized for the lowest smoke and NO emissions. The test engine was later operated at the optimized conditions and performance, combustion, and emission readings were recorded. The recorded readings were compared to that of a single injection of HRF with RCOB/hexanol. The future scope of the investigation would include the implementation of a similar strategy for automotive engines with an increased number of injections (>2).

## 2.MATERIALS AND METHODOLOGY

The current research seeks to optimise the operating parameters of an RCOB/Hexanol dual-fuel RCCI engine for lowest smoke and NO emissions at medium load (1.85 kW) operation. The work is built upon the previous work of the author (Thomas et al. 2020) and compares the effects of double injection of HRF over a single injection concerning combustion and emissions. The tests were performed on a single-cylinder water-cooled CI engine, utilised as a Genset. Since such an engine typically operates at part load, and to reduce the number of graphs, the present work only covers experimentation at medium load. Hexanol (LRF) was injected into the intake port at 3 bar $P_{inj}$ using a PFI system, during early suction stroke whereas RCOB (HRF) was injected directly into the combustion chamber during compression stroke by means of a common rail direct injection (CRDi) system at $P_{inj}$; 400, 500, and 600 bar. Intake air was maintained at a constant temperature of 40 °C and pressure of 1 bar. The LRF ratio was varied from 20 to 50 % while engine operating parameters such as HRF injection timings, injection quantity and pressure, as well as EGR quantity, were varied to optimize the engine operation for the lowest smoke and NO emissions. Combustion and emission data were collected for the engine operating at the optimized condition and were compared to data from a single injection (Thomas et al. 2020).

### 2.1. Test Engine

The tests were carried out on a Kirloskar AV1 single-cylinder CI engine. Table 1 contains the technical specifications for the test engine.

**Table 1: Technical details of the engine**

| | |
|---|---|
| Make | Kirloskar AV1 |
| Combustion chamber (mm x mm) | 80 x 110 |
| Engine speed (rpm) | 1500 |
| Displacement volume (cc) | 553 |
| Compression ratio | 16.5:1 |
| Rated power kW at rpm | 1.85 at 1500 |
| Connecting rod length (mm) | 235 |
| Bowl type | Hemispherical |
| Valve opening (°bTDC CA)* | |
| Inlet | 5 |
| Exhaust | -145 |
| Valve closing (°bTDC CA)* | |
| Inlet | 145 |
| Exhaust | -5 |

- = 0 ° CA corresponds to firing or compression TDC

The stock engine was altered to operate in RCCI mode. The low-pressure fuel injection system was replaced by a *Bosch* make CRDi system with a 6-hole solenoid injector for DI of HRF into the combustion chamber at higher $P_{inj}$ (400 to 600 bar). An additional low-pressure *Denso* make PFI system was also equipped to inject LRF (at 3 bar) into the intake manifold. An air preheater was utilized to maintain intake air constant at 40 °C and an automotive EGR unit was used to recirculate exhaust gases into the combustion chamber. Necessary sensors and measuring instruments such as *Bosch* cam sensor, *Kistler* crank angle encoder, *Kistler* pressure transducer, thermocouple, *Bosch* rail pressure sensor, and *Bosch* pressure control valve were used to control and maintain the engine operating parameters. The sensors and injectors were controlled using *National Instruments'* open ECU (*NI DIDS*). Pressure data was acquired with the help of a *Kistler* pressure transducer integrated with a *National Instruments'* data acquisition system (*NI DAQ*). The *NI DAQ* worked in conjecture with a *LabVIEW* based software which plotted and stored the pressure as well as crank angle data in real-time. The exhaust emissions were determined using an AVL 437c smoke metre and an AVL 444n di gas analyzer. AVL 444n DIGAS analyzer uses infrared measurement for CO, $CO_2$ and HC measurement whereas for $O_2$ and NO emissions it uses electrochemical measurement. AVL 437c smoke opacity meter detects and measures the amount of light blocked in the smoke emitted by diesel engines with the help of a halogen bulb and selenium photocell detector. The measurement device's accuracy and uncertainties are given in Table 2. The experimental engine is shown in Figure 1 complete with all required equipment.

## 2.2. Test Fuels

In the present work, RCOB and hexanol were employed as HRF and LRF, respectively. Both these renewable fuels are made from food/agro-industry waste. The hexanol used in the present

work was bought from Research Lab Chemicals, Pune, India. However, RCOB was produced in the laboratory at Anna University from RCO collected from the food court.

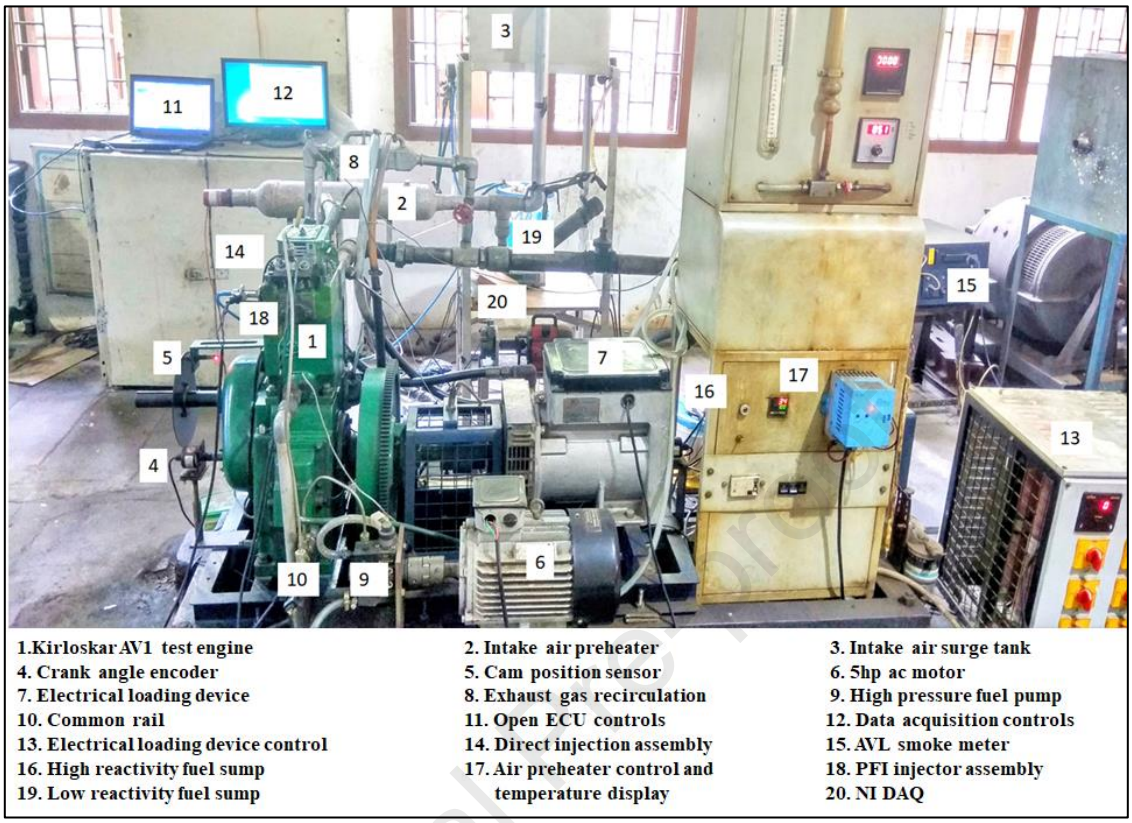


**Figure 1: Experimental rig with instrumentation**

**Table 2: Measurement devices range and accuracy**

| Measuring Device | Unit | Range | Accuracy |
|---|---|---|---|
| Speed Indicator | rpm | 0–5000 | ±1 |
| K type thermocouple | °C | 0–1000 | ±1 |
| AVL Di gas analyzer | | | |
| $CO_2$ | % of vol | 0–20 | ±0.5 |
| CO | % of vol | 0–10 | ±0.03 |
| HC | ppm | 0–20,000 | ±10 |
| NO | ppm | 0–5000 | ±50 |
| AVL 437c Smoke meter | % opacity | 0–100 | ±0.1% |
| Weighing balance for fuel measurement | kg | 0–10 | ±0.001 |

### 2.2.1 Biodiesel preparation

RCO was filtered using a sieving cloth and then with filter paper to remove any traces of dust or food particles. Thereafter the oil was titrated with 1N KOH solution to find the free-fatty acid percentage. Based on the titration, the trans-esterification process was selected for the

conversion of RCO to RCOB. Transesterification was carried out with methanol using KOH as a base catalyst (Thomas et al, 2020).

The process was carried out using a 5-litre pilot plant equipped with a heater, reflex condenser, and an electrically controlled stirrer. The oil was heated to 55 °C and methanol was added in a 4:1 molar ratio to the heated oil. KOH was utilized as the catalyst at a concentration of 1% by weight. The mixture was maintained at 60 °C for about 90 minutes and stirred at a speed of 60 rpm. After completion, the heater and stirrer were turned off and the mixture was transferred to a separating flask for overnight retention. The glycerol accumulated in the bottom and was subsequently removed. This glycerol was used for the manufacture of soap. To eliminate residues of glycerol, the oil was sprayed with hot distilled water. After washing the oil, it was heated to around 115-120 °C and maintained at that temperature for 15 minutes to remove moisture.

Basic properties of the test fuels were measured in the biodiesel lab of Anna University and others were taken from the literature (Kumar & Saravanan, 2016, Babu & Anand, 2017) as mentioned in Table 3.

**Table 3:** Test fuel properties compared to that of Diesel

| **Properties** | **RCOB** | **1-Hexanol** | **Diesel** |
|---|---|---|---|
| Molar mass | 250-260 | 102.18 | 190-211.7 |
| Density in kg/$m^3$ @ 15° C * | 875 | 822 | 836 |
| Kinematic viscosity in cSt @ 40 °C * | 4.75 | 3.33 | 2.4 |
| Net calorific value in MJ/kg | 39.7 | 39 | ≈43 |
| Enthalpy of vaporization in kJ/kg | - | 605 | < 305 |
| Cetane number | 58 | 24 | 46 |
| Fire point in °C * | 164 | 65 | 55 |
| Flash point in °C * | 159 | 58 | 47 |
| Iodine value ($gI_2$/ 100g) | 176 | - | - |
| Acid value (mg KOH/g) * | 0.44 | - | - |
| Oxygen (wt. %) | 11.98 | 15.70 | 0 |

* *= Measured quantity*

## 2.3. Methodology

Based on the previous study of the author it was observed that LTC combustion of hexanol and RCOB using a single injection and without EGR can significantly reduce NO and smoke emissions (Thomas et al, 2020). The engine was operated at medium load (1.85 kW) at 1500 rpm, for the duration of the research, with hexanol and RCOB as LRF and HRF respectively. The pressure-crank angle data were collected for an average of 120 cycles to account for cyclic variations. HRR was calculated from the pressure crank angle data based on the first law of thermodynamics. Hexanol was injected at constant 3 bar $P_{inj}$ and 5 °aTDC while RCOB injection parameters were varied parametrically to optimize the operation for lowest smoke and NO emissions. Initially, the experimental engine was operated using BDH30 (30% hexanol &

70% RCOB), based on a previous study (Thomas et al, 2020), and air temperature and pressure at intake were maintained constant at 40 °C and 1 atm. The amount of exhaust gas recirculated through the engine was increased from 10% to 30% in steps of 5 and the engine combustion and emission data were recorded. EGR was limited to 30% because any further increase in the proportion of exhaust gases hurt the engine combustion as well as increased the smoke emissions. The calculations for EGR were done by measuring the intake and exhaust $CO_2$ using Equation 1 given below.

$$EGR\ \% = \frac{CO_2\ in\ the\ intake}{CO_2\ in\ the\ exhaust} \text{ x } 100 \quad (1)$$

Thereafter, the RCOB injection parameters were optimized parametrically. Initially, the injection angles for pilot and main injections (SOI1 and SOI2) were varied maintaining the fuel injected at SOI1 and SOI2 constant. SOI1 injection angle was maintained at 45 °bTDC and SOI2 was varied from 11 to 17 °bTDC in steps of 2° CA. Later with SOI2 optimized for lowest NO and smoke emission, SOI1 was varied from 41 to 49 °bTDC in steps of 2° CA and the engine data were recorded. Once the injection angles were optimized, the fuel-injected during SOI1 and SOI2 were optimized by varying them from 30:70 (30% RCOB injected during SOI1 and 70% during SOI2) to 70:30 in steps of 10%. Thereafter with injection angles and quantity optimized for lowest smoke and NO emissions, the fuel $P_{inj}$ was changed from 400, 500 to 600 bar. Finally, the engine was operated at the optimized conditions with different fuel combinations, BDH20 to BDH50, and the combustion and emission data were gathered and compared to those obtained from LTC with a single injection and without EGR (Thomas et al, 2020). The comparisons are presented in Section 3. The operating conditions for the parametric study are summarized in Table 4. The uncertainties in measurement are provided in Table 5.

**Table 4**: Engine operating conditions for parametric study

| **Operating Parameters** | **Values** |
|---|---|
| Load (kW) | 1.85 |
| Engine speed (rpm) | 1500 |
| Intake air temperature (°C) | 40 |
| Intake air pressure (bar) | 1 |
| Hexanol $P_{inj}$ (bar) | 3 |
| Hexanol energy share | 30 |
| EGR rate (%) | 10, 15 ,20, 25, 30 |
| SOI1 timing (° bTDC ) | 49, 47, 45, 43, 41 |
| SOI2 timing (° bTDC ) | 17,15,13,11 |
| Fuel quantity at SOI1:SOI2 | 30:70, 40:60, 50:50, 60:40, 70:30 |
| SOI1 and SOI2 $P_{inj}$ (bar) | 400, 500, 600 |

**Table 5**: Uncertainty in measurement

| Parameter | Uncertainty (± %) |
|---|---|
| Engine speed | 0.14 |
| Fuel flow: | |
| Hexanol | 1.04 |
| Diesel | 1.1 |
| NO | 0.45 |
| HC | 0.65 |
| Smoke | 1.2 |
| CO | 0.61 |

## 3. RESULTS AND DISCUSSIONS

### 3.1. Effect of EGR on Combustion and Emissions

This section discusses the effects of exhaust gas recirculation on engine combustion and emissions. The test engine was operated on BDH30 (biodiesel 70% and hexanol 30%), based on a previous study of the author (Thomas et al, 2020). The exhaust gases introduced into the intake was varied from 10 to 30% in steps of 5. Figure 2(a) illustrates the cylinder pressure and HRR values for engine combustion at mid-load when the EGR rate is increased from 10% to 30%.

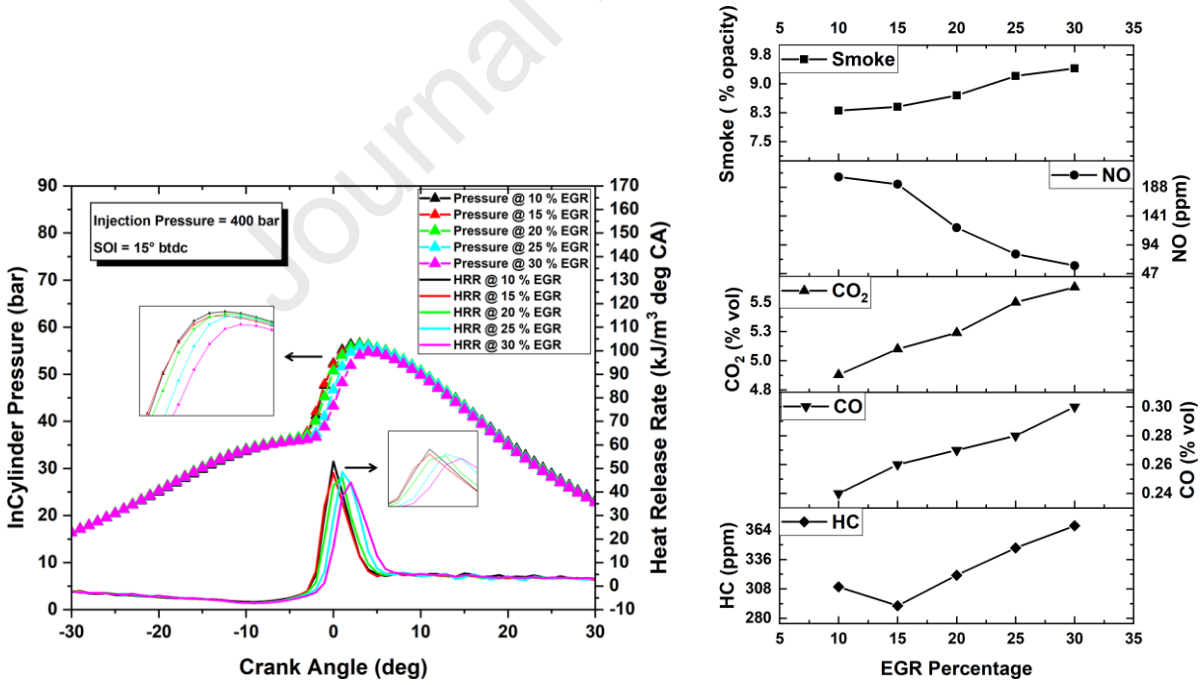


**(a)** **(b)**

**Figure 2:** (a) Pressure and HRR vs Crank angle (b) Emissions with increasing EGR

It is observed that when the proportion of EGR increases, the pressure curve shifts towards TDC. This is because when the amount of EGR increases, the cylinder temperature

decreases (Rajesh and Saravanan, 2015). Reduced cylinder temperature results in increased time for vaporisation and mixing, resulting in a delayed SOC (Kosmadakis *et al.*, 2019). Another point to note from Figure 2(a) is the reduction in pressure peak (57 bar to 54.5 bar) and HRR peak (53 to 44 kJ/m$^3$ deg CA) as the amount of exhaust gases increases. This tendency is due to EGR's dilution and heat capacity effects (Pundir, 2010). Due to the fact that exhaust gases replace $O_2$ in the mixture, combustion efficiency decreases. Furthermore, the specific heat of exhaust gases primarily $CO_2$ and $H_2O$ are high and therefore they absorb more heat from the surrounding compressed air and decrease the cylinder temperature (Rakopoulos *et al.*, 2020). As shown in Figure 2(a), the combined effect results in a decrease in pressure and HRR peaks.

The increase in exhaust gases from 10% to 30% results in an increase in smoke output. Smoke emissions increase from 8.3 to 9.4 (% vol) as the exhaust gases substitute fresh air from the cylinder. As shown in Figure 2(b), EGR is an efficient technique for reducing NO emissions. NO emission was substantially decreased (from 205 to 60 ppm) when the EGR proportion was increased from 10 to 30 %. $CO_2$ emissions increased marginally from 4.9 to 5.6 (% vol). EGR is basically the recirculation of $CO_2$ and $H_2O$ from the exhaust back into the combustion chamber, and as the proportion of EGR increases, $CO_2$ emissions rise, as shown in Figure 2(b). The increase in CO emission (from 0.24 to 0.3 (% vol)) associated with increased EGR may be attributed to the decrease in the cylinder temperature associated with increased EGR, implying that CO oxidation to $CO_2$ is not complete (Rakopoulos *et al.*, 2018). As shown in Figure 2(b), HC emissions increase gradually from 310 to 368 ppm with an increase in EGR flow rate. The higher HC emission is caused by a reduction in cylinder temperature and a decrease in combustion efficiency. With 25% exhaust gases recirculated, the engine emissions were observed to be the lowest.

### 3.2. Effect of Double injection on Combustion and Emissions

The effects of SOI1 and SOI2 timings, fuel amount injected at SOI1 and SOI2 (SOI1:SOI2), and $P_{inj}$ of SOI1, SOI2 on combustion and emissions during mid-load operation are shown in Figures 4 to 8. SOI1 was initially set to 45 °bTDC CA while SOI2 was changed from 17 and 11 °bTDC CA. The ratio of fuel injected at SOI1 to SOI2 was constant at 50:50. As presented in Figure 3(a), when the injection angle of SOI2 is delayed or retarded (moved towards TDC) from 17 °bTDC to 11 °bTDC, there is a decrease in peak pressure as well as HRR peak, and both the curves shift towards TDC. Peak pressure reduced from 60.5 to 54 bar whereas HRR peak reduced from 24.5 to 11.5 kJ/m$^3$ deg CA. With a further delay in SOI2, at 9 °bTDC engine starts to misfire as presented in Figure 4. As the injection is delayed, the cylinder temperature and pressure rise, which should enhance combustion via improved atomization and mixing. However, before the combustion can complete, the piston returns to the bottom dead centre, and the cylinder temperature and pressure fall (Pundir, 2010). As a result, it exhibits poor engine performance and combustion efficiency (Yesilyurt *et al.*, 2018). The same trend can be observed in the HRR as well. As the SOI2 moves towards the TDC, the HRR peak reduces and shifts towards the right as depicted in Figure 3(a). The Low-temperature reaction (LTR) region is also visible which is the heat release due to SOI1 and is depicted by the small first peak in the HRR diagram (Vallinayagam *et al.*, 2017).

As SOI2 is retarded from 17 °bTDC, smoke emissions decrease from 3.5 to 2.8 (% vol) (Figure 3(b)). This is because, at late compression stroke, the compression temperature and pressure are higher. This leads to finer droplets of injected fuel which evaporates faster and therefore results in lower smoke emission (Wei *et al.* 2014). NO emission also decreases with delayed SOI2 (280 to 127 ppm), because NO emission is temperature dependant and as exhibited in Figure 3(a), HRR and therefore cylinder temperature reduces with delayed SOI2.

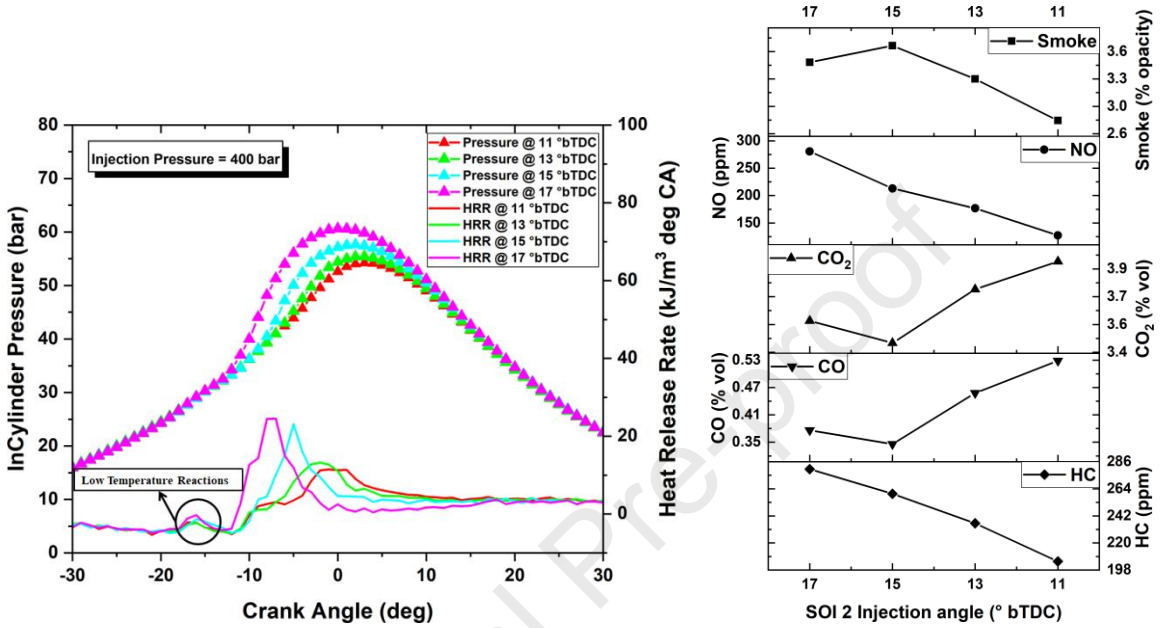


**Figure 3: Variation in combustion and emission curves with SOI2 injection timings**

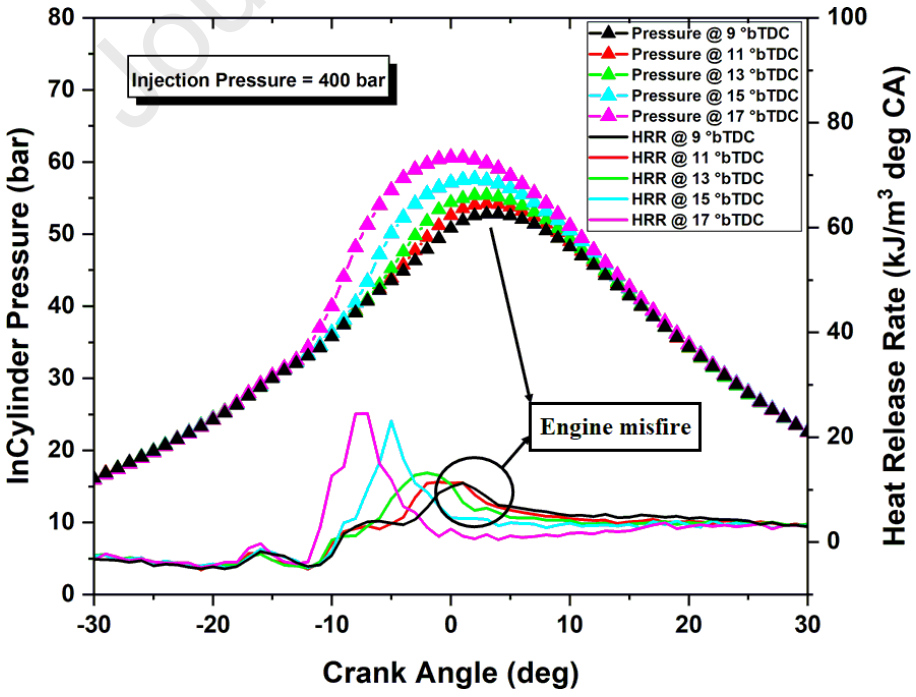


**Figure 4: Engine misfire with delayed SOI2 at 9 °bTDC**

Since the combustion quality deteriorates as SOI2 is retarded, more fuel is injected to compensate for the power loss (Akcay *et al.*, 2020), this leads to an increase in $CO_2$ emission from 3.6 to 4 (% vol) as shown in Figure 3(b). CO emission also increases (0.38 to 0.53 (% vol)) as a consequence of poor combustion efficiency and reduced cylinder temperature. Higher compression pressure and temperature as the SOI2 delays, lead to the smaller droplet size of injected fuel as well as lesser wall impingement since the cylinder pressure is higher, this results in a drop in HC emission from 280 to 205 ppm (Qian *et al.*, 2019).

From the experimental outcome, SOI2 at 13 °bTDC was fixed and SOI1 was varied. SOI1 was advanced from 41 °bTDC to 49 °bTDC as presented in Figure 5(a). It can be observed that with advancing SOI1, the pressure curve retards and peak pressure reduces. The peak pressure drops from 59 to 57 bar. This is because, with advanced SOI1, the compression pressure and temperature are lower and with the injection of fuel, the temperature further drops down because of the higher specific heat of the fuel (Jatoth *et al.*, 2021). This leads to retarded SoC and therefore the curves shift towards TDC and hence the drop in peak pressure. From the HRR curve it is observed that at SOI1 of 41 °bTDC, the compression temperature is high enough in such a way that it forms a combustible mixture by SOI2 and therefore combustion starts immediately as perceived from Figure 5(a). Whereas with advanced SOI1, the compression temperature drops, and therefore, the heat release is delayed. With SOI2 at 13 °bTDC, the rise in HRR is slowed down as observed in the figure as the plateau region. The combustion, therefore, starts a few crank angle degrees later by that time all the fuel (entrained hexanol and RCOB) burn together, and therefore HRR increases.

Figure 5(b) illustrates the impact of advanced SOI1 on emission. Smoke emissions rise from 3 to 8.3 (% vol) with advanced SOI1 due to reduced compression temperature and pressure, which results in wall impingement and bigger droplet size, as well as slower vaporisation and mixing (Janbarari & Ahmadian, 2020). This also explains the increase in HC emission from 269 to 415 ppm with advanced SOI1. At 41 °bTDC SOI, the compression temperature is high enough for the start of combustion almost immediately after SOI2, but as SOI1 is further advanced, the compression temperature drops. From 41 °bTDC to 45 °bTDC, the NO emission decreases (203 to 173 ppm) due to inefficient combustion.

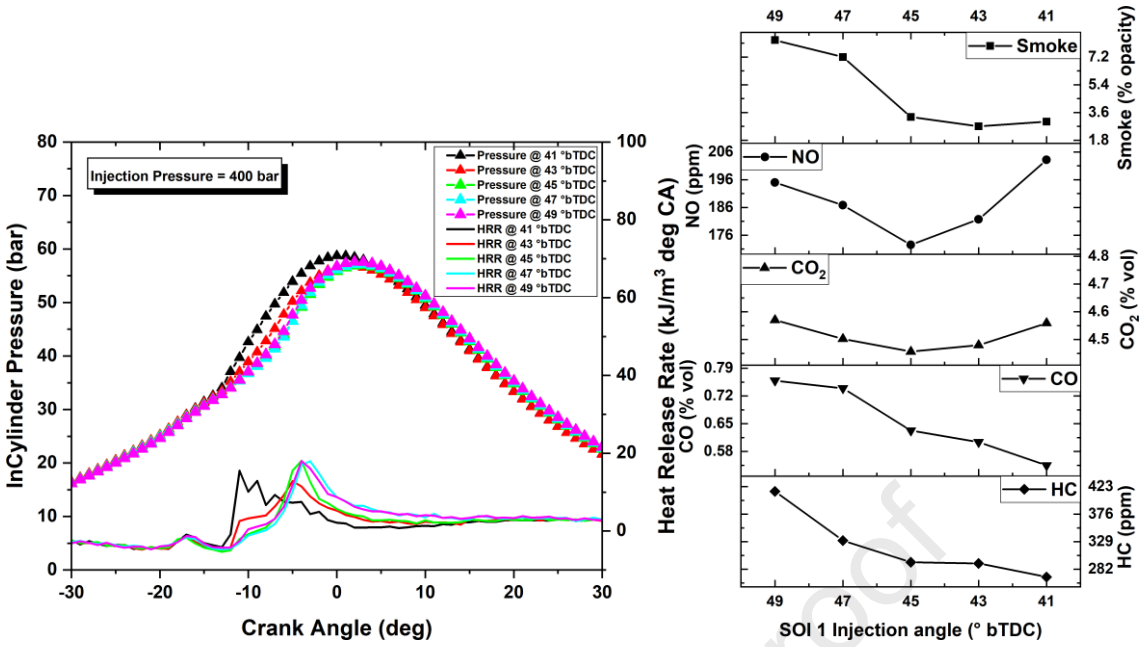


**(a)** **(b)**

**Figure 5: Variation in combustion and emission curves with SOI1 injection timings**

As the SOI further advances, because of lower temperature, the ID or lag increases, therefore more fuel is accumulated and combustion of that fuel leads to an increase in NO emissions from 173 to 195 ppm (Borah *et al.*, 2018) as observed in Figure 5(b). Advanced SOI1 has no effect on $CO_2$ emissions, however, CO emissions rise (from 0.54 to 0.76 (% vol)) as a consequence of inefficient combustion..

SOI1 was set to 45 °bTDC based on testing findings, and the proportion of fuel injected during SOI1 and SOI2 was adjusted. The fuel injection ratio in SOI1:SOI2 was changed between 30:70 and 70:30, as shown in Figure 6(a). With an increase in the proportion of SOI1 injection quantity from 30% to 70 %, it is observed that the pressure and HRR curve advances as well as peak pressure and HRR peak increases. The peak pressure increased from 53 to 67 bar whereas the HRR peak increased from 25 to 67 kJ/m$^3$ deg CA. Increased quantity of fuel in SOI1 means more fuel mixes with air and makes a combustible mixture by the time of SOI2 and therefore more fuel takes part in the premixed stage of combustion resulting in a higher peak (Giakoumis *et al.*, 2016) as observed in Figure 6(a), which could lead to engine knocking. With a very high quantity of SOI1 injection, it is observed that the peak shifts before TDC, which results in an increased compression work. With an increased quantity of SOI2 injection, more and more fuel takes part in diffusion combustion instead of premixed combustion, therefore the peaks are lower as observed from the HRR diagram in Figure 6(a).

As shown in Figure 6(b), increasing the percentage of SOI1 fuel from 30% to 70% results in a decrease in smoke output from 7.1 to 3.8 (% vol). This is because more quantity of fuel forms a homogenous combustible mixture with air resulting in fewer fuel-rich zones and

therefore fewer smoke emissions (Sharma *et al.*, 2019). NO emissions increase from 169 to 433 ppm with an increased SOI1 fraction. The large quantity of premixed fuel mixture results in higher heat release and therefore increased NO emission as perceived from Figure 6(b). This increased temperature also leads to a rise in $CO_2$ emission and a drop in CO emission from 30% SOI1 to 70% SOI1. $CO_2$ increases from 4.1 to 5.3 (% vol) whereas CO reduces from 0.68 to 0.55 (% vol). Higher fuel injection quantity early in the compression stroke when compression temperature is lower leads to increased HC emission (233 to 309 ppm) as a result of increased wall impingement (Zehni *et al.*, 2017).

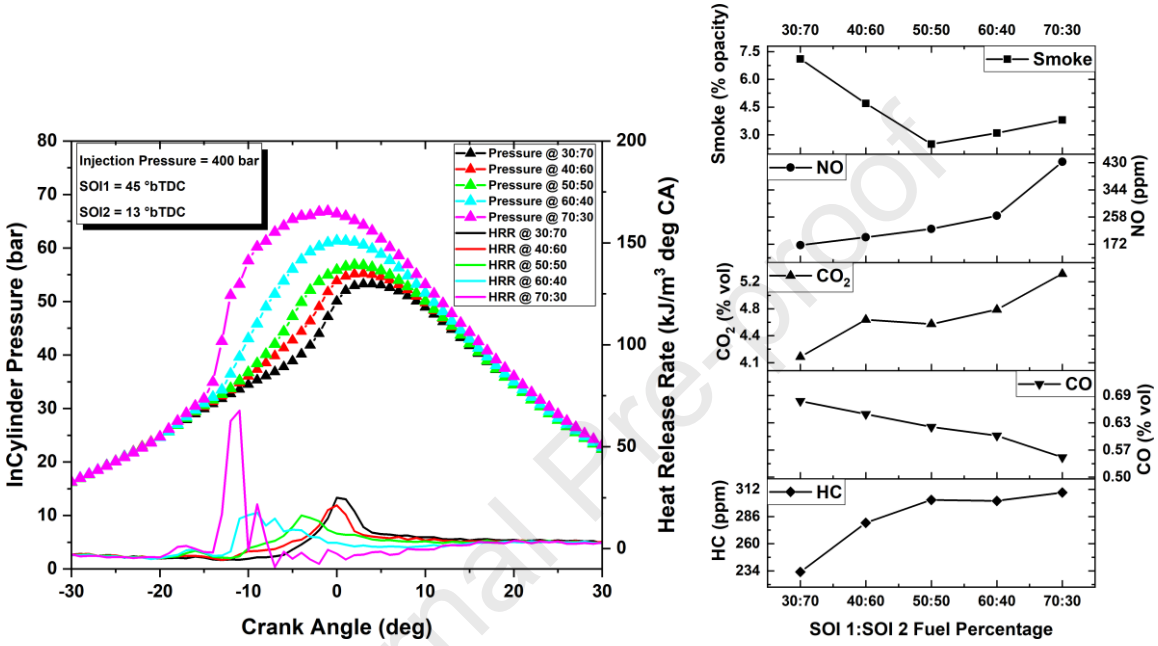


**(a)** **(b)**

**Figure 6: Variation in combustion and emission curves with SOI1:SOI2 injection quantities**

The 50:50 ratio of SOI1 to SOI2 fuel quantity was selected for further testing in order to achieve reduced emissions. Now, with SOI1 set to 45 °bTDC, SOI2 set to 13 °bTDC, and the SOI1:SOI2 injection ratio set to 50:50, the fuel $P_{inj}$ was altered to investigate the effect on engine combustion and emission. The combustion pressure and HRR curves for 400, 500, and 600 bar Pinj at mid-load are shown in Figure 7(a). As Pinj rises, the ID increases, which may be attributed to wall impingement and therefore a delay in the onset of combustion. More fuel accumulated during ignition lag results in a higher peak in HRR (from 15 to 54 kJ/m$^3$ deg CA) as portrayed in Figure 7(a).

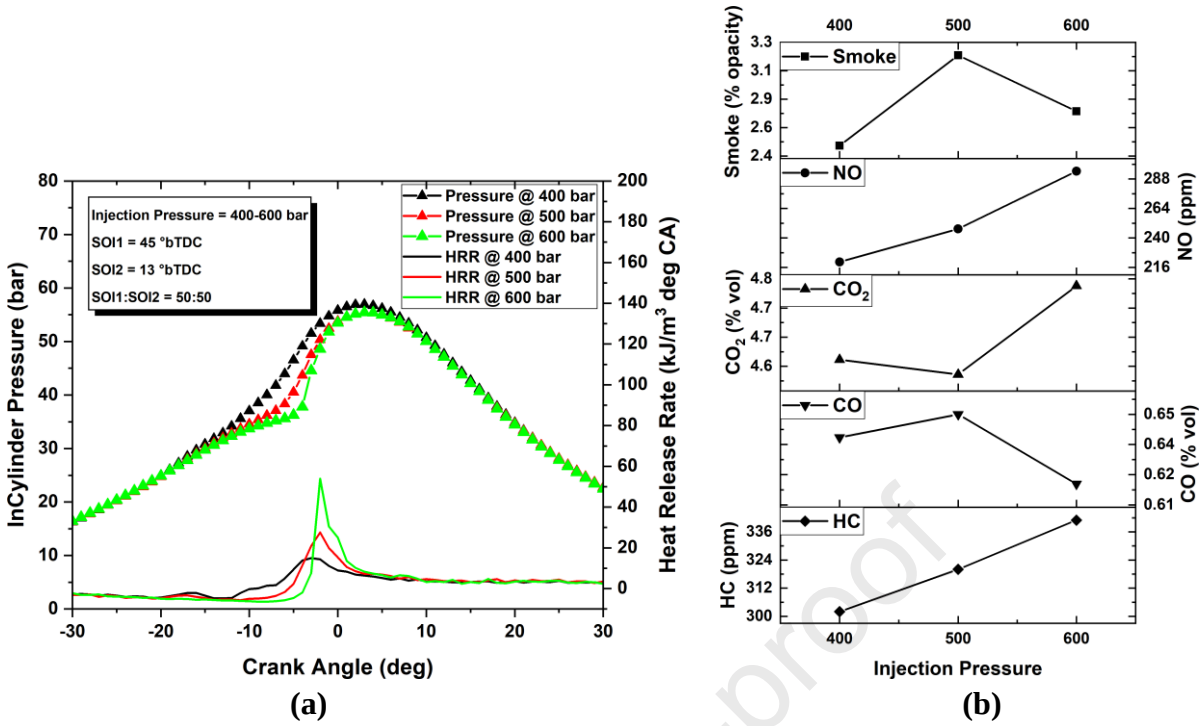


**Figure 7: Variation in combustion and emission curves with HRF injection pressure**

Figure 7(b) shows that when $P_{inj}$ increases smoke emissions increase marginally from 2.5 to 3.2 (% vol), which could be because of the retarded combustion. NO emission is temperature dependant and with an increase in temperature as evident from Figure 7(a), NO increase with increasing $P_{inj}$ from 220 to 294 ppm. Additionally, increased temperature results in greater conversion of CO to $CO_2$, resulting in increased $CO_2$ emissions (4.6 to 4.8 (% vol)) and decreased CO emissions (0.64 to 0.62 (% vol)). Higher wall impingement at higher $P_{inj}$ and lower load conditions could be the reason for increased HC emission (302 to 341 ppm) as perceived from Figure 7(b). The lowest NO emission is observed at a $P_{inj}$ pressure of 400 bar.

### 3.3. Comparison with Single Injection

With the exhaust gas quantity and fuel injection parameters optimized experimentally for the lowest possible emissions, the collected combustion and emission data for the optimized operation were compared to those of a single HRF injection as well as Diesel to ascertain the advantages of double injection in reducing smoke and NO emissions. Table 6 summarises the optimal operating conditions.

**Table 6: Engine operation conditions for comparative study**

| Operating Parameters | Values |
|---|---|
| EGR rate (%) | 25 |
| SOI1 (° bTDC) | 45 |
| SOI2 (° bTDC) | 13 |

| | |
|---|---|
| SOI1 to SOI2 fuel quantity | 50:50 |
| $P_{inj}$ (bar) | 400 |
| Hexanol energy share | 20,30,40,50 |

### 3.3.1. Cylinder Pressure and HRR

The comparison of cylinder pressure and HRR for double injection with a single injection as well as diesel combustion is shown in Figure 8.

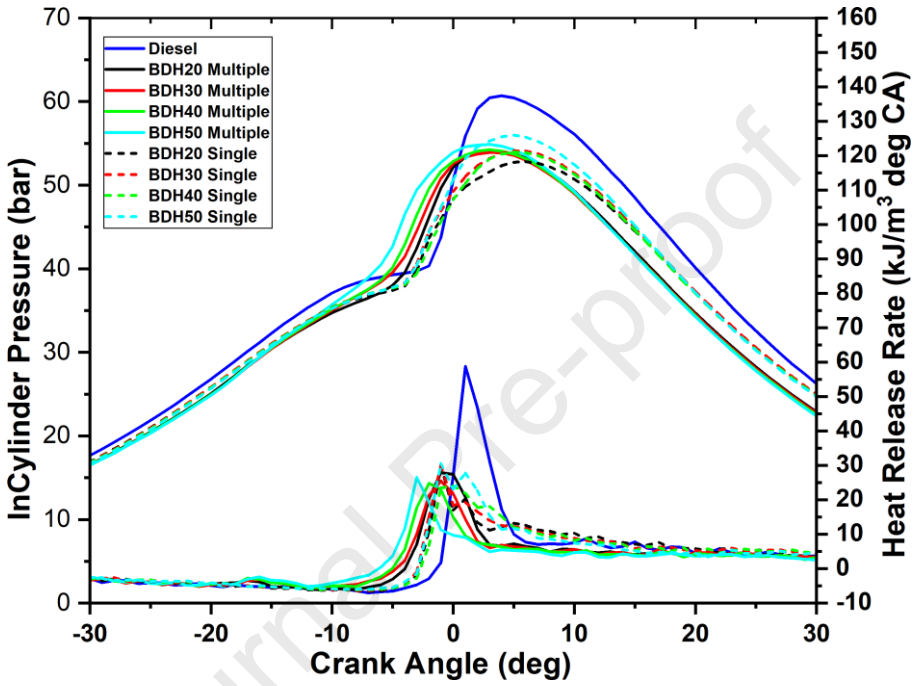


**Figure 8: Pressure and HRR for single injection compared to that of double injection**

As shown in the figure, the pressure and HRR for BDH combinations (both single injection and double injection) (52-56 bar) are lower than that of Diesel (60.5 bar) which may be ascribed to the lower energy density of both RCOB and hexanol in comparison to Diesel. However higher cetane number of RCOB and advanced injection angle results in advanced SOC of BDH combination compared to that of Diesel. Double injection of RCOB increases the pressure and HRR curves relative to a single injection due to the advanced injection angle (45 °bTDC CA). There is only a marginal difference between pressure and HRR peaks of single and double injection with double injection peaks (54-55 bar) marginally lower than for single injection (53-56 bar). This may be because the premixed combustion phase is shorter for double injection as the air-fuel mixture is available for combustion by SOI2 because of earlier injection (SOI1 at 45 °bTDC) (Papagiannakis *et al.*, 2017).

### 3.3.2. Combustion Parameters

The combustion parameters such as the start of combustion (SOC), ignition delay (ID) are critical for comprehending the combustion process within the engine cylinder. Figure 9

shows the comparisons for SOC and ID between single injection and double injection of RCOB in dual-fuel operation. SOC and ID were calculated by plotting mass fraction burnt.

The start of combustion is considered as the crank angle at which 10% of the fuel has been consumed (Sharma *et al.*, 2019). From Figure 9(a), it can be observed that SOC is advanced for double injection (2-4 °bTDC) than that for a single injection (0.5-2 °bTDC). This is because of advanced injection at 45 °bTDC CA compared to single injection at 15 °bTDC. When the fuel is injected in advance (SOI1), sufficient time is available for the formation of the combustible mixture, and therefore with a second injection (SOI2) the physical delay is reduced and this leads to a shorter premixed combustion phase (Papagiannakis *et al.*, 2017). It can also be understood from Figure 9(a) that with an increase in the percentage of LRF from 20% to 50% the SOC also advances marginally. This is due to an increase in in-cylinder temperature caused by improved combustion in the presence of higher oxygen in the premixed charge (Rakopoulos *et al.*, 2018).

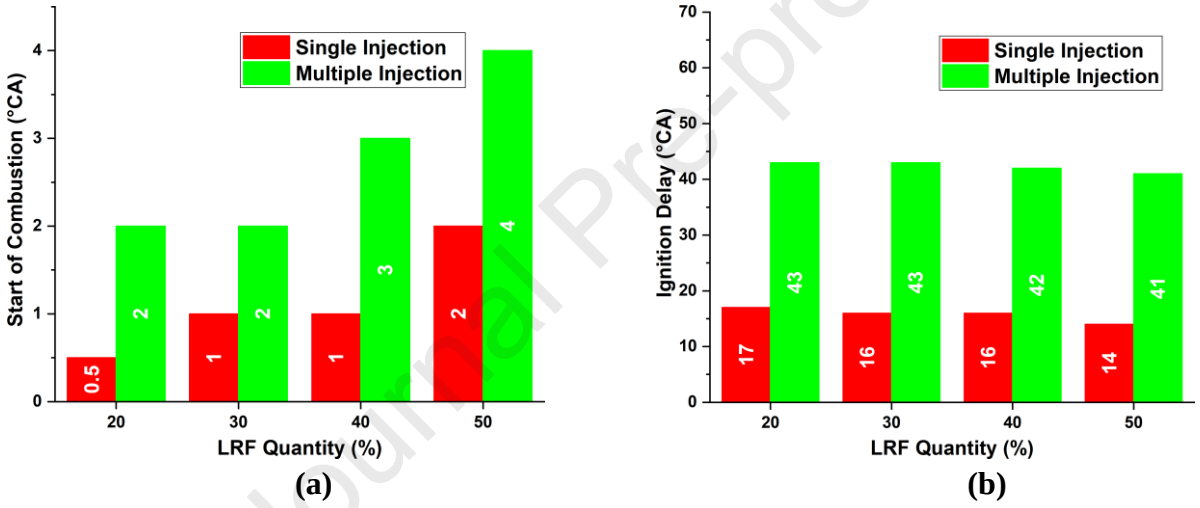


**Figure 9: Combustion parameters for single and double injection of HRF**

Figure 9(b) shows the comparison of ID between single injection and double injection of RCOB. Here ID is taken as the time gap in crank angle degrees between the start of injection and the start of combustion (Sharma *et al.*, 2019). Since the fuel is injected earlier in the compression stroke (45 °bTDC) for double injection, the ID is considerably large (41 to 43 °bTDC) compared to single injection (14-17 °bTDC) for all BDH combinations. This increased ID helps in the preparation of a better air-fuel mixture which helps in the reduction of smoke emissions (Thomas *et al.*, 2021). However, with the increase in the percentage of LRF, ID reduces for both single injection and double injection as can be observed from Figure 9(b). This is due to an increase in in-cylinder temperature as a consequence of improved combustion in the presence of higher fuel-bound oxygen.

### 3.3.3. Emissions

The exhaust emissions for single injection and double injection are compared with that of Diesel operation and are presented in Figure 10.

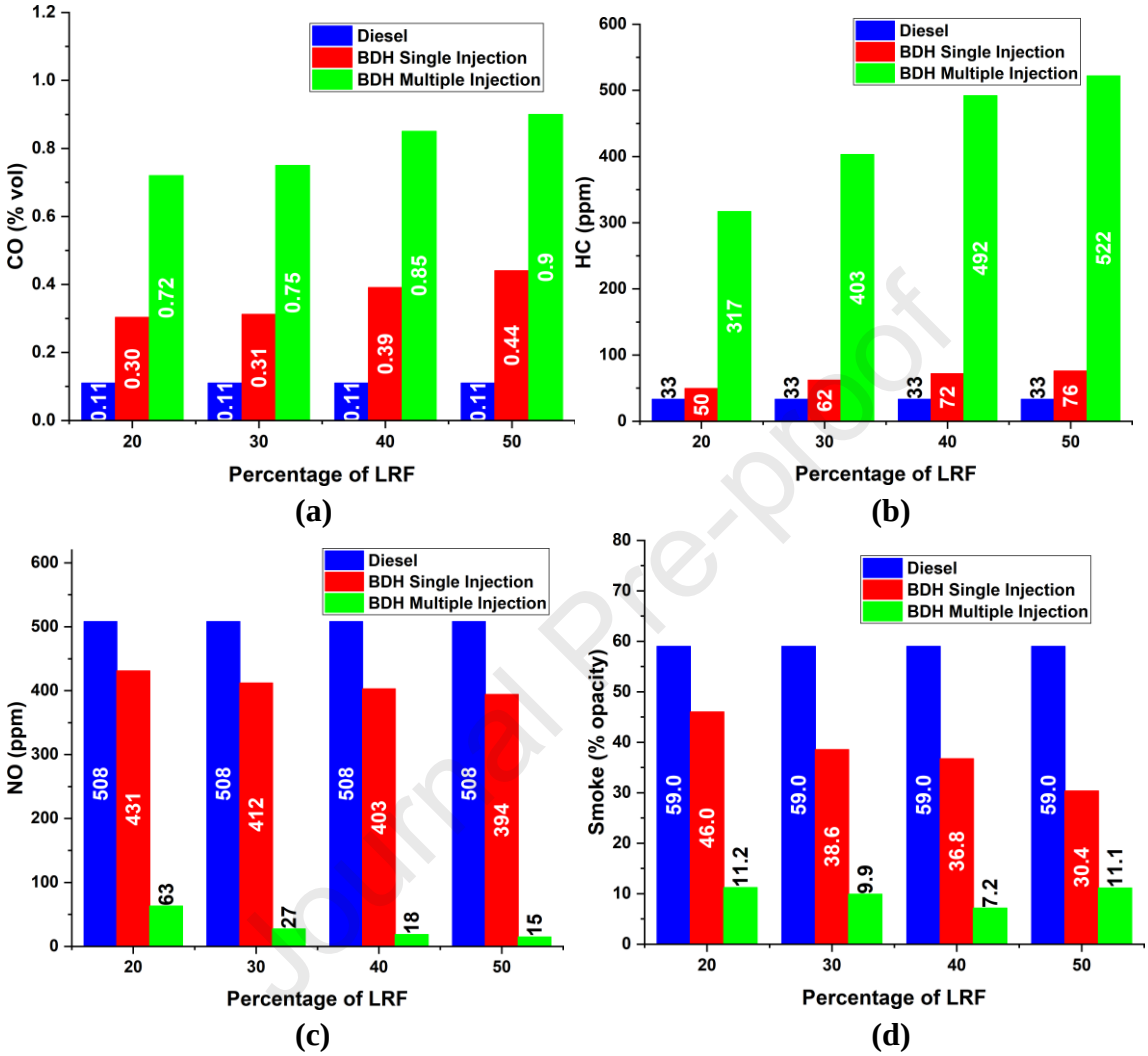


**Figure 10: Comparison of exhaust emissions for single and double injection**

It is observed from Figure 10(a) that CO emissions have increased for RCCI (0.3-0.9 (% vol)) combustion compared to that of Diesel (0.11 (% vol)) as an outcome of LTC. Oxidation of CO to $CO_2$ is hindered because of the low temperature (Guan *et al.*, 2014). It can also be noticed that with an increase in the percentage of LRF from 20 to 50 %, CO emissions increase for both single injection (0.3-0.44 (% vol)) and double injection (0.72-0.9 (% vol)) which could be due to the cooling effect of hexanol (Thomas *et al.*, 2021). The CO emissions for double injection are comparatively higher than single injection. This could be attributed to lower in-cylinder temperature because of increased amount premixed charge as well as increased $O_2$ concentration earlier in the compression stroke. The HC emissions for RCCI combustion with single injection as well as double injection are compared to Diesel combustion (33 ppm) as observed from Figure 9(b). HC emissions are higher in the case of double injection (317-522 ppm) which is credited to the lower in-cylinder temperature as well as an advanced

injection during earlier compression stroke that results in wall wetting and improper oxidation (Zehni *et al.*, 2017). As the proportion of LRF increases (Figure 10 (b)), these HC emissions rise further due to hexanol's greater latent heat of vaporisation.

There is a concurrent reduction in smoke and NO emissions for both single injection and double injection when compared to Diesel injection as observed from Figure 10 (c) and (d) because of the LTC and improved mixing and evaporation leading to improved premixed combustion phase (Zehni *et al.*, 2017). The reduction in NO (from 508 to 15 ppm), as well as smoke emission (from 59 to 7.2 (% vol)), is higher for double injection because of earlier injection which provides more time for preparation of the combustible mixture (Rakopoulos et al., 2018). With the increase in the percentage of LRF, oxygen content increases which lead to better oxidation of soot particles, and the reduced temperature as a result of the cooling effect of hexanol hinders the NO production (Rahman *et al.*, 2013).

### 3.3.4. Efficiency

Thermal efficiency measures how effectively the heat energy provided to the engine by the chemical energy in the fuel is transformed into productive work (Qian *et al.*, 2019). The indicated thermal efficiency for single injection and double injection are compared and shown in Figure 11.

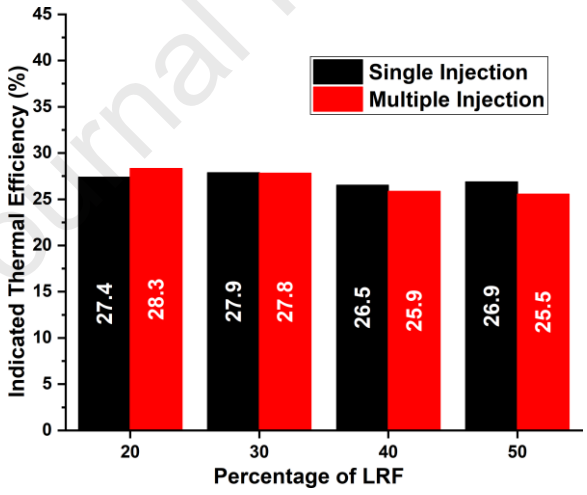


**Figure 11: Comparison of indicated thermal efficiency for single injection and double injection**

It is observed from Figure 11 that the indicated thermal efficiency is higher for double injection at a lower LRF fraction, however, as the proportion of hexanol increases, efficiency reduces compared to a single injection of RCOB. This is due to the lower in-cylinder temperature caused by the advanced injection during an earlier compression stroke, as well as the cooling action of hexanol (Thomas *et al.*, 2021). Thermal efficiency decreases as the LRF proportion increases for both single and repeated injections, due to hexanol's greater latent heat

of vaporisation. Maximum improvement in thermal efficiency is at 20% LRF fraction (BDH20) and is equal to 0.9 %.

## 4. CONCLUSIONS

The single-cylinder water-cooled CI was operated at mid-load in dual-fuel RCCI mode using direct injection of RCOB and PFI of hexanol. The double injection of RCOB was experimentally optimized for the lowest emission by optimizing the injection parameters such as injection timing, injection quantity, and injection pressure in addition to the amount of exhaust gas recirculated into the engine combustion chamber. Later the engine was operated at the optimized condition. The data collected from the optimized operation was compared to dual-fuel operation with a single injection of RCOB based on the author's previous work (Thomas et al, 2020). The following conclusions were drawn from the parametric study and comparisons made between single and double injection:

1. EGR is an effective NO reduction technique. With an increase in the percentage of exhaust gases recirculated (from 10 to 30%) into the combustion chamber, NO emissions reduced by 70%, however other emissions increased; smoke (13.2%), CO (25%), $CO_2$ (14.3%), and HC (18.7%). A drop in peak pressure was also noticed with the increasing EGR rate.
2. Fuel injection is critical for compression ignition, smoke and NO emissions reduced by 20 and 56.4% respectively with late main injection (17 to 13 °bTDC CA) whereas smoke increased by 2.7 times and NO reduced by 14.7% with advanced pilot injection (41 to 49 °bTDC CA); NO increased with pilot injection advanced beyond 45 °bTDC CA. Concerning engine performance, peak pressure dropped by 9% with late main injection and 3.3% with advanced pilot injection.
3. With increased SOI1 injection quantity (from 30to 70 %), smoke decreased by 46.5% whereas NO increased by 2.5 times, however, when $P_{inj}$ rose from 400 to 600 bar, both smoke and NO emissions increased by 28% and 33% respectively. With regard to performance peak pressure increased by 26.4% with pilot injection quantity.
4. Compared to a single injection of RCOB, a maximum reduction of 96% in NO and an 80% reduction in smoke emissions were observed with the double injection of RCOB and 25% EGR. Additionally, there is a marginal increase in thermal efficiency (~1%). However, peak pressure dropped by about 7.4% and CO and HC emissions increased as is typical with LTC.

Thus, RCOB and Hexanol generated from agricultural waste can be effectively used in dual-fuel LTC to simultaneously reduce NO and smoke emissions with a marginal increase in thermal efficiency. Being carbon-neutral fuels, this would also reduce net $CO_2$ emissions. The promotion of these biofuels would empower the agricultural economy and help the farmer in operating farm equipment and vehicles using these fuel generated from the farm waste. It would also promote small scale industries and business establishments in the rural area to setup production plant and sell the fuel conveniently.

**ACKNOWLEDGEMENT**

The authors extend their gratitude to Centre for Research, Anna University, Chennai, India, for granting the ACRF fellowship, Lr. No. CFR/ACRF/2017/3, during January 2017-December 2019, which was supportive for conducting the research.

**REFERENCES**

[1] Aboelazayem O, Gadalla M, Saha B. Valorisation of high acid value waste cooking oil into biodiesel using supercritical methanolysis: Experimental assessment and statistical optimisation on typical Egyptian feedstock. Energy 2018;162:408–20. https://doi.org/10.1016/j.energy.2018.07.194

[2] Akcay M, Yilmaz IT, Feyzioglu A. Effect of hydrogen addition on performance and emission characteristics of a common-rail CI engine fueled with diesel/waste cooking oil biodiesel blends. Energy 2020;212:118538. https://doi.org/10.1016/j.energy.2020.118538

[3] Atmanli A. Comparative analyses of diesel-waste oil biodiesel and propanol, n-butanol or 1-pentanol blends in a diesel engine. Fuel 2016;176:209–15. https://doi.org/10.1016/j.fuel.2016.02.076

[4] Babu D, Anand R. Effect of biodiesel-diesel- n -pentanol and biodiesel-diesel- n -hexanol blends on diesel engine emission and combustion characteristics. Energy 2017;133:761–76. https://doi.org/10.1016/j.energy.2017.05.103.

[5] Benajes J, García A, Monsalve-Serrano J, Villalta D. Exploring the limits of the reactivity controlled compression ignition combustion concept in a light-duty diesel engine and the influence of the direct-injected fuel properties. Energy Convers Manag 2018;157:277–87. https://doi.org/10.1016/j.enconman.2017.12.028

[6] Benajes J, Molina S, García A, Monsalve-Serrano J. Effects of direct injection timing and blending ratio on RCCI combustion with different low reactivity fuels. Energy Convers Manag 2015;99:193–209. https://doi.org/10.1016/j.enconman.2015.04.046

[7] Benajes J, Molina S, García A, Monsalve-Serrano J. Effects of low reactivity fuel characteristics and blending ratio on low load RCCI (reactivity controlled compression ignition) performance and emissions in a heavy-duty diesel engine. Energy 2015:1–11. https://doi.org/10.1016/j.energy.2015.06.088

[8] Borah MJ, Devi A, Saikia RA, Deka D. Biodiesel production from waste cooking oil catalyzed by in-situ decorated TiO2 on reduced graphene oxide nanocomposite. Energy 2018;158:881–9. https://doi.org/10.1016/j.energy.2018.06.079

[9] Campos-fernández J, Arnal JM, Gómez J, Dorado MP. A comparison of performance of higher alcohols / diesel fuel blends in a diesel engine 2012;95:267–75. https://doi.org/10.1016/j.apenergy.2012.02.051

[10] Chaitanya VS, 'Air pollution in Delhi Essay – Case Study'. 2017; Available from: https://www.kitchenarena.in/delhi-air-pollution/

[11] Curran SJ, Hanson RM, Wagner RM. Reactivity controlled compression ignition combustion on a multi-cylinder light-duty diesel engine. Int J Engine Res 2012;13:216–25. https://doi.org/10.1177/1468087412442324

[12] Dempsey AB, Ryan Walker N, Reitz R. Effect of piston bowl geometry on dual fuel reactivity controlled compression ignition (RCCI) in a light-duty engine operated with gasoline/diesel and methanol/diesel. SAE Int J Engines 2013;6:78–100. https://doi.org/10.4271/2013-01-0264

[13] García A, Monsalve-Serrano J, Martinez-Boggio S, Gaillard P, Poussin O, Amer AA. Dual fuel combustion and hybrid electric powertrains as potential solution to achieve 2025 emissions targets in medium duty trucks sector. Energy Convers Manag 2020;224:113320. https://doi.org/10.1016/j.enconman.2020.113320

[14] Gharehghani A, Hosseini R, Mirsalim M, Jazayeri SA, Yusaf T. An experimental study on reactivity controlled compression ignition engine fueled with biodiesel/natural gas. Energy 2015;89:558–67. https://doi.org/10.1016/j.energy.2015.06.014

[15] Giakoumis EG, Rakopoulos DC, Rakopoulos CD. Combustion noise radiation during dynamic diesel engine operation including effects of various biofuel blends: A review. Renewable and Sustainable Energy Reviews 2016;54:1099–113. https://doi.org/10.1016/j.rser.2015.10.129

[16] Goel S, Sharma R, Kumar A. A review on barrier and challenges of electric vehicle in India and vehicle to grid optimisation, Transportation Engineering 2021;4. https://doi.org/10.1016/j.treng.2021.100057

[17] Guan B, Zhan R, Lin H, Huang Z. Review of state of the art technologies of selective catalytic reduction of NOx from diesel engine exhaust. Appl Therm Eng 2014;66:395–414. https://doi.org/10.1016/j.applthermaleng.2014.02.021

[18] Guan C, Cheung CS, Ning Z, Wong PK, Huang Z. Comparison on the effect of using diesel fuel and waste cooking oil biodiesel as pilot fuels on the combustion, performance and emissions of a LPG-fumigated compression-ignition engine. Appl Therm Eng 2017;125:1260–71. https://doi.org/10.1016/j.applthermaleng.2017.07.117

[19] Janbarari SR, Ahmadian Behrooz H. Optimal and robust synthesis of the biodiesel production process using waste cooking oil from different feedstocks. Energy 2020;198:117251. https://doi.org/10.1016/j.energy.2020.117251

[20] Jatoth R, Gugulothu SK, Ravi kiran Sastry G. Experimental study of using biodiesel and low cetane alcohol as the pilot fuel on the performance and emission trade-off study in the diesel/compressed natural gas dual fuel combustion mode. Energy 2021;225:120218. https://doi.org/10.1016/j.energy.2021.120218

[21] Karabektas M, Hosoz M. Performance and emission characteristics of a diesel engine using isobutanol–diesel fuel blends. Renew Energy 2009;34(6):1554–9. http://dx.doi.org/10.1016/j.renene.2008.11.003

[22] Kokjohn SL, Hanson RM, Splitter DA. Rietz RD. Fuel Reactivity controlled compression ignition (RRCI): a pathway to controlled high efficiency clean combustion. International Journal of Engine Research 2011;12(3):209-226 https://doi.org/10.1177/1468087411401548

[23] Kokjohn SL, Reitz RD. Reactivity controlled compression ignition and conventional diesel combustion: a comparison of methods to meet light-duty NOx and fuel economy targets. Int J Engine Res 2013;14:452–68. https://doi.org/10.1177%2F1468087413476032

[24] Kosmadakis GM, Rakopoulos DC, Rakopoulos CD. Performance and emissions of a methane-fueled spark-ignition engine under consideration of its cyclic variability by using a computational fluid dynamics code. Fuel 2019;258:116154. https://doi.org/10.1016/j.fuel.2019.116154

[25] Kumar BR, Saravanan S, Rana D, Nagendran A. A comparative analysis on combustion and emissions of some next generation higher-alcohol / diesel blends in a direct-injection diesel engine. Energy Convers Manag 2016;119:246–56. https://doi.org/10.1016/j.enconman.2016.04.053

[26] Li J, Yang WM, An H, Zhao D. Effects of fuel ratio and injection timing on gasoline/biodiesel fueled RCCI engine: A modeling study. Appl Energy 2015;155:59–67. https://doi.org/10.1016/j.apenergy.2015.05.114

[27] Lu X, Jian-Guang Y, Wu-Gao Z, Zhen H. Effect of cetane number improver on heat release rate and emissions of high speed diesel engine fueled with ethanol-diesel blend fuel. Fuel 2004;83:2013–20. https://doi.org/10.1016/j.fuel.2004.05.003

[28] Ma Y, Huang R, Huang S, Zhang Y, Xu S, Wang Z. Experimental investigation on the effect of n-pentanol blending on spray, ignition and combustion characteristics of waste cooking oil biodiesel. Energy Convers Manag 2017;148:440–55. https://doi.org/10.1016/j.enconman.2017.06.027

[29] Mohsin R, Majid ZA, Shihnan AH, Nasri NS, Sharer Z. Effect of biodiesel blends on engine performance and exhaust emission for diesel dual fuel engine. Energy Convers Manag 2014;88:821–8. https://doi.org/10.1016/j.enconman.2014.09.027

[30] Papagiannakis RG, Krishnan SR, Rakopoulos DC, Srinivasan KK, Rakopoulos CD. A combined experimental and theoretical study of diesel fuel injection timing and gaseous fuel/diesel mass ratio effects on the performance and emissions of natural gas-diesel HDDI engine operating at various loads. Fuel 2017;202:675–87. https://doi.org/10.1016/j.fuel.2017.05.012

[31] Pundir BP, I C Engines: Combustion and Emissions, Narosa Publishing House, 2010, ISBN 978-81-8487-087-9.

[32] Qian Y, Chen F, Zhang Y, Tao W, Han D, Lu X. Combustion and regulated/unregulated emissions of a direct injection spark ignition engine fueled with C3-C5 alcohol/gasoline surrogate blends. Energy 2019;174:779–91. https://doi.org/10.1016/j.energy.2019.03.021

[33] Qian Y, Wang X, Zhu L, Lu X. Experimental studies on combustion and emissions of RCCI (reactivity controlled compression ignition) with gasoline/n-heptane and ethanol/n-heptane as fuels. Energy 2015;88:584–94. https://doi.org/10.1016/j.energy.2015.05.083

[34] Rahman SMA, Masjuki HH, Kalam MA, Abedin MJ, Sanjid A, Sajjad H. Impact of idling on fuel consumption and exhaust emissions and available idle-reduction technologies for diesel vehicles - A review. Energy Convers Manag 2013;74:171–82. https://doi.org/10.1016/j.enconman.2013.05.019

[35] Rajesh B, Saravanan S. Effect of exhaust gas recirculation ( EGR ) on performance and emissions of a constant speed DI diesel engine fueled with pentanol / diesel blends. Fuel 2015;160:217–26. https://doi.org/10.1016/j.fuel.2015.07.089

[36] Rajesh Kumar B, Saravanan S. Use of higher alcohol biofuels in diesel engines: A review. Renew Sustain Energy Rev 2016;60:84–115. https://doi.org/10.1016/j.rser.2016.01.085.

[37] Rakopoulos CD, Rakopoulos DC, Kosmadakis GM, Papagiannakis RG. Experimental comparative assessment of butanol or ethanol diesel-fuel extenders impact on combustion features, cyclic irregularity, and regulated emissions balance in heavy-duty diesel engine. Energy 2019;174:1145–57. https://doi.org/10.1016/j.energy.2019.03.063

[38] Rakopoulos CD, Rakopoulos DC, Mavropoulos GC, Kosmadakis GM. Investigating the EGR rate and temperature impact on diesel engine combustion and emissions under various injection timings and loads by comprehensive two-zone modeling. Energy 2018;157:990–1014. https://doi.org/10.1016/j.energy.2018.05.178

[39] Rakopoulos DC, Rakopoulos CD, Giakoumis EG, Papagiannakis RG. Evaluating Oxygenated Fuel's Influence on Combustion and Emissions in Diesel Engines Using a Two-Zone Combustion Model. Journal of Energy Engineering 2018;144:04018046. https://doi.org/10.1061/(asce)ey.1943-7897.0000556

[40] Rakopoulos DC, Rakopoulos CD, Kosmadakis GM, Giakoumis EG. Exergy assessment of combustion and EGR and load effects in DI diesel engine using comprehensive two-zone modeling. Energy 2020;202:117685. https://doi.org/10.1016/j.energy.2020.117685

[41] Ramos TRP, Gomes MI, Barbosa-Póvoa AP. Planning waste cooking oil collection systems. Waste Manag 2013;33:1691–703. https://doi.org/10.1016/j.wasman.2013.04.005

[42] Reijnders J, Boot M, de Goey P. Impact of aromaticity and cetane number on the soot-NOx trade-off in conventional and low temperature combustion. Fuel 2016; 186: 24–34, https://doi.org/10.1016/j.fuel.2016.08.009

[43] Sharma AR, Kharol SK, Badarinath KVS, Singh D. Impact of agriculture crop residue burning on atmospheric aerosol loading - A study over Punjab State, India. Ann Geophys 2010;28:367–79. https://doi.org/10.5194/angeo-28-367-2010

[44] Sharma V, Duraisamy G, Muk H, Arumugam K, M AA. Production , combustion and emission impact of bio-mix methyl ester fuel on a stationary light duty diesel engine. J Clean Prod 2019;233:147–59. https://doi.org/10.1016/j.jclepro.2019.06.003.

[45] The Hindu. India's percentage CO2 emissions rose faster than the world average, available at https://www.thehindu.com/news/national/indias-percentage-co2-emissions-rose-faster-than-the-world-average/article33965283.ece, [accessed on 26th January 2022]

[46] Thomas JJ, Nagarajan G. Residual Cooking Oil Biodiesel and Hexanol as Alternatives to Petroleum-Based Fuel in Low- Temperature Combustion: Parametric Study 2021:1–14. https://doi.org/10.4271/2021-01-0520.Abstract.

[47] Thomas JJ, Sabu VR, Basrin G, Nagarajan G. Hexanol: A renewable low reactivity fuel for RCCI combustion. Fuel 2020;286:119294. https://doi.org/10.1016/j.fuel.2020.119294

[48] Thomas JJ, Sabu VR, Nagarajan G, Kumar S, Basrin G. Influence of waste vegetable oil biodiesel and hexanol on a reactivity controlled compression ignition engine combustion and emissions. Energy 2020;206:118199. https://doi.org/10.1016/j.energy.2020.118199

[49] Tsoutsos T, Tournaki S, Gkouskos Z, Paraíba O, Giglio F, García PQ, et al. Quality characteristics of biodiesel produced from used cooking oil in Southern Europe. ChemEngineering 2019;3:1–13. https://doi.org/10.3390/chemengineering3010019.

[50] Vallinayagam R, Vedharaj S, An Y, Dawood A, Izadi Najafabadi M, Somers B, et al. Compression Ignition of Light Naphtha and Its Multicomponent Surrogate under Partially Premixed Conditions 2017. https://doi.org/10.4271/2017-24-0078.

[51] Victor M, Sathiyagnanam AP, Rana D, Rajesh Kumar B, Saravanan S. 1-Hexanol as a sustainable biofuel in DI diesel engines and its effect on combustion and emissions under the influence of injection timing and exhaust gas recirculation (EGR). Appl Therm Eng 2017;113:1505–13. https://doi.org/10.1016/j.applthermaleng.2016.11.164

[52] Wallace T, Gibbons D, O'Dwyer M, Curran TP. International evolution of fat, oil and grease (FOG) waste management – A review. J Environ Manage 2017;187:424–35. https://doi.org/10.1016/j.jenvman.2016.11.003.

[53] Wei L, Cheng R, Mao H, Geng P, Zhang Y, You K. Combustion process and NOx emissions of a marine auxiliary diesel engine fuelled with waste cooking oil biodiesel blends. Energy 2018;144:73–80. https://doi.org/10.1016/j.energy.2017.12.012

[54] Wiznia D, Ellis H and Geist G (2006) 'Biofuels Implementation and Emission Analysis'. A Thesis.

[55] Yesilyurt MK, Eryilmaz T, Arslan M. A comparative analysis of the engine performance, exhaust emissions and combustion behaviors of a compression ignition engine fuelled with biodiesel/diesel/1-butanol (C4 alcohol) and biodiesel/diesel/n-pentanol (C5 alcohol) fuel blends. Energy 2018;165:1332–51. https://doi.org/10.1016/j.energy.2018.10.100

[56] Zehni A, Khoshbakhti Saray R, Poorghasemi K. Numerical comparison of PCCI combustion and emission of diesel and biodiesel fuels at low load conditions using 3D-CFD models coupled with chemical kinetics. Appl Therm Eng 2017;110:1483–99. https://doi.org/10.1016/j.applthermaleng.2016.09.056.

[57] Zhong Y, Han W, Jin C, Tian X, Liu H. Study on effects of the hydroxyl group position and carbon chain length on combustion and emission characteristics of Reactivity Controlled Compression Ignition (RCCI) engine fueled with low-carbon straight chain alcohols. Energy 2022;239:122259. https://doi.org/10.1016/j.energy.2021.122259

HIGHLIGHTS

- Hexanol-Residual cooking oil biodiesel in low-temperature combustion
- Double injection strategy to reduce emissions
- Reduction in nitric oxide emission by 96% and smoke emission by 80%
- Peak pressure drop by 7.4% compared to Diesel combustion
- Improvement in thermal efficiency by 1% compared to single injection

**Declaration of interests**

☒ The authors declare that they have no known competing financial interests or personal relationships that could have appeared to influence the work reported in this paper.

☐The authors declare the following financial interests/personal relationships which may be considered as potential competing interests: